Natural Resources Research (© 2019)
https://doi.org/10.1007/s11053-019-09596-0

Original Paper

Prediction of Reservoir Temperatures Using Hydrogeochemical Data, Western Anatolia Geothermal Systems (Turkey): A Machine Learning Approach

Fusun S. Tut Haklidir[1,3] **and Mehmet Haklidir**[2]

Received 8 April 2019; accepted 18 November 2019

Geothermal fluids can be used for purposes such as power production, district heating/cooling, agriculture, and industrial and thermal tourism. Although using geothermal fluids is beneficial, it requires detailed exploration studies of a region. These exploration studies mainly involve geology, geophysics and geochemistry disciplines to understand the location, dimensions, possible capacity and temperature of a reservoir before beginning drilling operations. Because of the high operational costs, the exploration phase of a geothermal project is of great importance to reduce project costs. Evaluation of existing earth sciences data, detailed geology studies, mapping and some geochemical studies, such as using geothermometers, can provide information about a potential geothermal reservoir in a geothermal field. Machine learning is a technology for data analysis which identifies patterns in data and uses them to make predictions about new data points automatically. In this study, a deep learning model is developed to predict geothermal reservoir temperatures based on selected hydrogeochemistry data from different geothermal systems. Two traditional regression approaches, linear regression and linear support vector machine, are performed to compare the prediction performance of our proposed deep learning model. The objective of the study is to obtain the algorithm having the lowest root-mean-square error and mean absolute error. The results show that the deep neural network (DNN) algorithm generated the lowest errors. The DNN model provided the most accurate values close to geothermometer calculations for reservoir temperature. The performance comparison showed that our deep learning model achieved the best prediction performance compared to traditional machine learning techniques.

KEY WORDS: Machine learning, Deep learning, Hydrogeochemistry, Reservoir temperature prediction, Geothermal exploration.

INTRODUCTION

Geothermal energy is stored at depth in the earth. It has many areas of use depending on the temperature of the fluids. These fluids mainly consist of hot water, steam and gases, which can be utilized for electricity production, space heating and cooling, agricultural and industrial applications and balneology purposes (Fig. 1). Some of these applications require low–medium-temperature geofluids, while electricity and district heating and cooling applications require medium–high temperatures.

[1]Department of Energy Systems Engineering, Istanbul Bilgi University, Eyüp, Istanbul, Turkey.
[2]TUBITAK BILGEM, Gebze, Kocaeli, Turkey.
[3]To whom correspondence should be addressed; e-mail: fusun.tut@bilgi.edu.tr

Published online: 27 November 2019

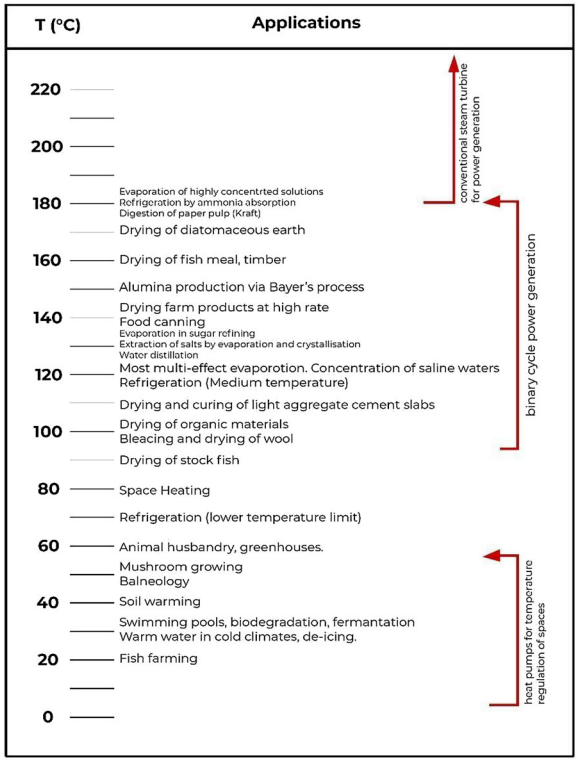

Figure 1. Geothermal energy applications (modified after Lindal 1973).

Sometimes it is not easy to reach geothermal sources at surface conditions, and different geothermal exploration studies are required to understand the characterization of a geothermal system. These can include temperature, potential, characterization of geofluids and determination of drilling locations prior to drilling operations in a field. The scientific disciplines for geothermal exploration are commonly related to geology, geochemistry and geophysics. Geology aims to understand the rock units, tectonics and volcanological evaluation and hydrological regime of a geothermal system. Geophysical studies help to determine the form, volume and depth of the heat source (Ochieng 2013), reservoir and cap rocks, while geochemistry provides possible reservoir temperatures, possible scale precipitations (Haklidir Tut and Haklidir 2017), chemistry of the geofluids and water–rock interaction at depth by stable isotopes such as δ18O and δD (Haklidir Tut 2013). All these disciplines are quite important to provide the required information to select the best drilling location and depth before a geothermal drilling operation.

Estimation of geothermal reservoir temperature is a critical issue for geothermal exploration, and geothermometers are commonly used for calculations to predict the geothermal reservoir temperature based on hydrogeochemical characterization of surface waters and springs in a geothermal system. Thermal springs may provide important clues to reach high reservoir temperatures in a geothermal field. Geothermometers may be classified as chemical, isotope or gas; these are all important geochemical indicators for the exploration of geothermal resources. These geothermometers help scientists to understand specific mineral-solute reactions, which are slow to re-equilibrate at different temperatures, especially under conditions where the fluid is effectively separated from the minerals which control the equilibria (Karingithi 2009). In particular, chemical geothermometers such as silica and cation geothermometers (such as Na–K and Na–K–Ca) are commonly used for the determination of reservoir temperatures at the liquid phase during a geothermal exploration survey (Arnorsson 2000). Using different geothermometers may provide the most correct prediction of reservoir temperature. However, these geothermometers have some limitations in different conditions and are not applicable for all geothermal sources.

Cold water mixing and the water–rock interaction status of geothermal sources are quite important for understanding which geothermometer is more reliable for a certain geothermal source (Karingithi 2009; Haklidir Tut 2013). For example, the Kızıldere and Tekkehamam geothermal fields belong to the same geothermal system in the Denizli region in Western Anatolia, Turkey. One thermal spring discharges in Tekkehamam (K5 spring) and has similar chemical analysis results as the KD-13 geothermal well in Kızıldere, which has a depth of 760 m and reservoir temperatures near 196 °C (Zorlu 2009). During the geothermal exploration studies in Kızıldere field, geothermometer calculations provided useful information about the reservoir conditions before the start of drilling operations in the field. In some cases, hydrochemical analysis, especially isotope and gas analysis of all geothermal fluids in a field, might be expensive in the first phase of the project development. Application of a different or innovative method to provide correction of reservoir temperature could be a good solution for a large geothermal field.

The use of machine learning (ML) for geothermal energy and geosciences is still developing. ML involves a wide range of technologies applied to a wide range of subjects in different fields. The development of ML technology for geothermal energy is expected to provide significant possibilities for using new technologies and cost reduction during the project life cycle, from geothermal exploration to power plant operations for geothermal investments. Advanced exploration studies using ML techniques for geological, geochemical, geophysical and geothermal research provide relevant information regarding geothermal energy. There are limited literature references to applications of ML technology for geothermal energy. Important studies include those by Rezvanbehbahani et al. (2017), who predicted heat flux in Greenland, and by Holtzman et al. (2018), who studied seismic source spectra in Geysers geothermal field. A new study by Haklidir Tut and Haklidir (2019), which examines fluid temperature prediction through hydrochemical data, emphasizes the data quality required for ML studies on reservoirs.

ML is a technology that can predict results based on a model prepared by training input data and output behavior. The developed model can be used to predict geothermal reservoir temperatures based on the existing hydrogeochemical data for geothermal fluids. In this study, thermal springs and high-temperature geothermal wells are used to build a dataset, as these represent the different geothermal systems in Western Anatolia. A performance comparison of ML algorithms was carried out, and the results are presented here.

GEOTHERMAL FLUIDS CHARACTERIZATION FOR HIGH- AND LOW-TEMPERATURE GEOTHERMAL SYSTEMS IN WESTERN ANATOLIA (TURKEY)

The Alpine–Himalayan orogenic belt was an important phenomenon in Turkey. The main tectonic zones, including the North Anatolian Fault, the Eastern Anatolian Fault and the Aegean Graben Systems, were formed in this belt. Turkey also has young volcanoes such as Kula (Manisa city) in Western Anatolia and Nemrut (Bitlis city) in Eastern Anatolia (Bozkurt 2001; Haklidir Tut 2013). All these geological activities are conducive to geothermal systems reaching different temperatures in this belt. More than 230 geothermal fields have been discovered in Turkey, and geothermal exploration studies continue throughout the country (Haklidir Tut 2017). Because of its extension zone and large graben systems, the highest reservoir temperatures can be found in Western Anatolia. This region is quite suitable for geothermal power production and district heating applications. The geopower capacity was approximately 1.5 GWe in 2019, provided by 45 geothermal power plants along large graben systems such as Büyük Menderes Graben and Gediz Graben (Fig. 2) (Haklidir Tut 2017). There are also more than 2900 MWt district heating applications in Western Anatolia (TJD 2018). The water–rock interaction in thermal waters is apparently more intense in Western Anatolia than in the other parts of the Turkey, which refers to higher water temperatures (Fig. 2).

High-Temperature Geothermal Systems in Western Anatolia

Most of the discovered high-temperature systems in Western Anatolia are situated in Part II of Figure 2a. The region has been strongly affected by the Aegean Extension Zone, and the crust tends to be thinner, which allows geothermal fluids to reach shallower depths than in the other areas shown in Figure 2a. Therefore, the heat flow in this zone is higher than in other parts of Western Anatolia (Şalk et al. 2005). The second important geothermal zone is located in Gediz Graben in the Part II region (Bundschuh et al. 2013). Water-dominated reservoir temperatures range from 180 to 245 °C (Fig. 3; Haklidir Tut and Şengün 2020), and this range of temperatures permits the use of different power cycles, even multi-flash systems (such as double flash, triple flash) and an advanced geothermal system (flash + binary) in the Büyük Menderes Graben (Haklidir Tut 2015). These large graben zones are also quite suitable for geothermal combine systems, as power production and district heating with 260 MWe of 1.4 GWe total installed power production and 50 MWt district heating application have been developed in the Kızıldere (Denizli city) geothermal field (Haklıdır Tut and Şengün 2020). In addition to Kızıldere Pamukören, the Salavatlı, Germencik (Aydın city) and Alasehir (Manisa city), high-temperature geothermal fields are shown in Part II of Figure 2a. One high-temperature geothermal system

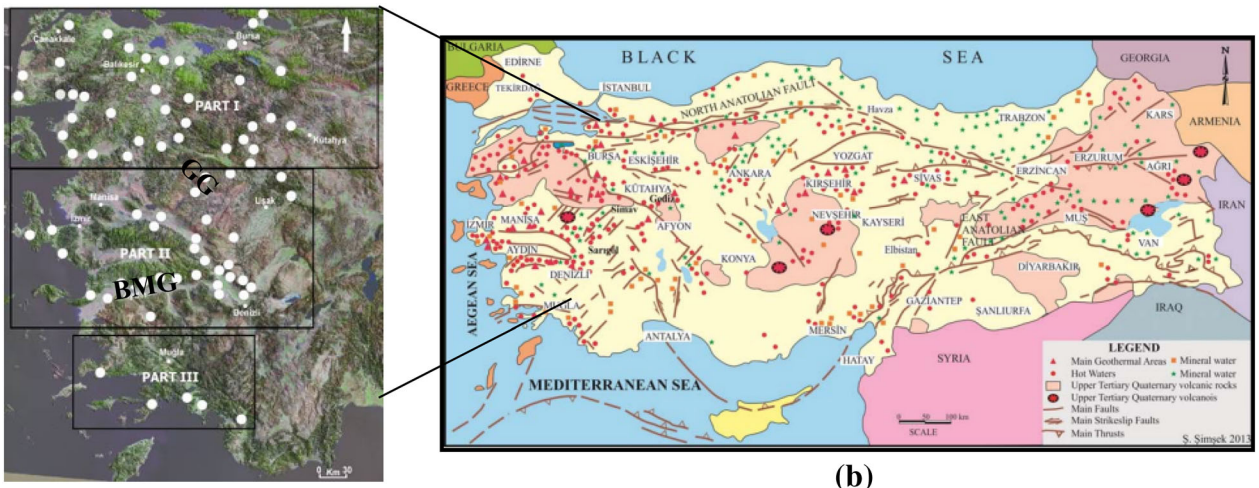

Figure 2. (**a**) Geothermal systems in Western Anatolia. Part I mainly represents medium–low-temperature systems, Part II represents high–medium-temperature systems and Part III represents low-temperature systems. *BMG* Büyük Menderes Graben. *GG* Gediz Graben. (**b**) Geothermal systems and hot springs in Turkey (Parlaktuna et al. 2013).

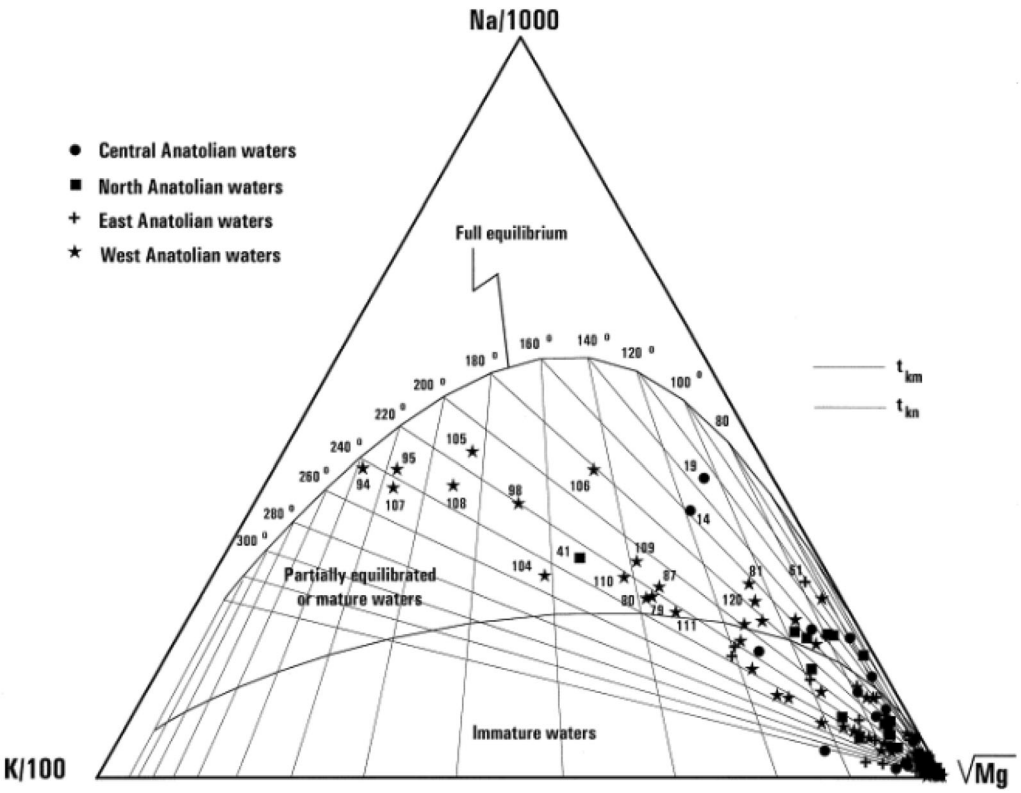

Figure 3. Water–rock interaction in thermal waters in Turkey (Mutlu and Güleç 1998).

(Tuzla) also exists in the western edge of Part I (Baba et al. 2015; Topçu et al. 2019).

Medium–Low-Temperature Geothermal Systems in Western Anatolia

If reservoir temperatures are less than 180 °C, an organic Rankine cycle (ORC) binary system generates steam more efficiently in water-dominated geothermal systems. An ORC binary system in a region is compact, requires less area and involves easier equipment installation than does a flash cycle power plant. There are more than 30 ORC binary geothermal power plants with capacities between 8MWe and 24 MWe, in addition to the flash-type steam turbine systems in the Part II region of Western Anatolia (Fig. 2a). The first ORC binary power plant started operations with 8.5 $MWe_{total\ gross}$ at the Dora-I plant in Salavatlı town (Aydın city) in 2006. In an ORC system, organic working fluids such as n-butane, n-pentane or a mixture were to produce superheated steam (DiPippo 2012). Other ORC binary plants are located in the Pamukören, Salavatlı and Germencik regions along the Büyük Menderes Graben, and Alasehir on the Gediz Graben (Haklidir Tut 2017). There are two ORC-binary-type power plants installed in Tuzla (Çanakkale), located in Part I of Figure 2a. The reservoir temperature has been recorded at around 170 °C in the Tuzla region in the north of Western Anatolia (Topçu et al. 2019; Karadas and Akkurt 2014). Different district heating and cooling applications are realized in Balçova, Bergama (İzmir city), Edremit, Gönen (Balıkesir city), Salihli (Manisa city) in the Part I and Part II regions of Figure 2a. Water temperatures can range between 60 and 140 °C (TJD 2018), which are higher-than-required values for district heating applications (Fig. 1).

LOW-TEMPERATURE GEOTHERMAL SYSTEMS IN WA

Thermal springs with temperatures lower than 75 °C are widely observed in Western Anatolia. These springs may be used for a few direct applications (Fig. 1). However, these are evaluated as good clues to reach higher temperatures during the geothermal exploration phase. Almost all geothermal exploration activities start with observing these thermal springs in a field before a detailed investigation of a geothermal field. Reservoir temperature estimations are important at this stage, and silica geothermometers in particular may give good results for prediction of reservoir temperature. Silica geothermometers provide more consistent results for shallow and low-temperature thermal springs because of their cold water mixing or precipitation effects (Haklidir Tut 2013). Low-temperature thermal springs are located at the edge of small grabens or fault zones such as the Bursa and Balıkesir regions in Part I of the study area (Fig. 2a).

METHODOLOGY

Machine Learning Approach

ML, as a subset of artificial intelligence, generally uses statistical techniques to allow computers to learn from the data available without being explicitly programmed (Samuel 1959). ML is a technology for data analysis, which identifies patterns in data and uses the identified patterns to automatically make predictions about new data points. Thus, one of the important applications of ML is prediction. There are two main types of ML: supervised and unsupervised. In the supervised learning, the dataset includes output classes used to train the machine. In the unsupervised learning, output class information is not available; instead, the data are partitioned into unknown classes (Russell and Norvig 2010). Supervised ML is adopted in this study to predict reservoir temperatures in geothermal systems.

Supervised learning can be described as follows: If there are input variables (X) and output variables (Y), an algorithm is used to learn the mapping function from input to output; thus, $Y = f(X)$. The aim is to approximate the mapping function so that if there are new input data (X), the output variables (Y) for these data can be predicted (Russell and Norvig 2010). Deep learning is an advanced ML, which can automatically learn representations from data without hand-coded rules or domain knowledge.

We propose a deep learning model, namely a deep neural network (DNN), to predict geothermal reservoir temperatures based on selected hydrogeochemistry data from different geothermal systems (Fig. 4). A DNN is an artificial neural network with a series of hidden layers between the input and

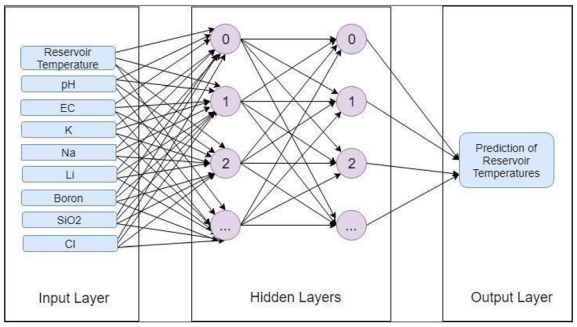

Figure 4. Proposed architecture of DNN in this study.

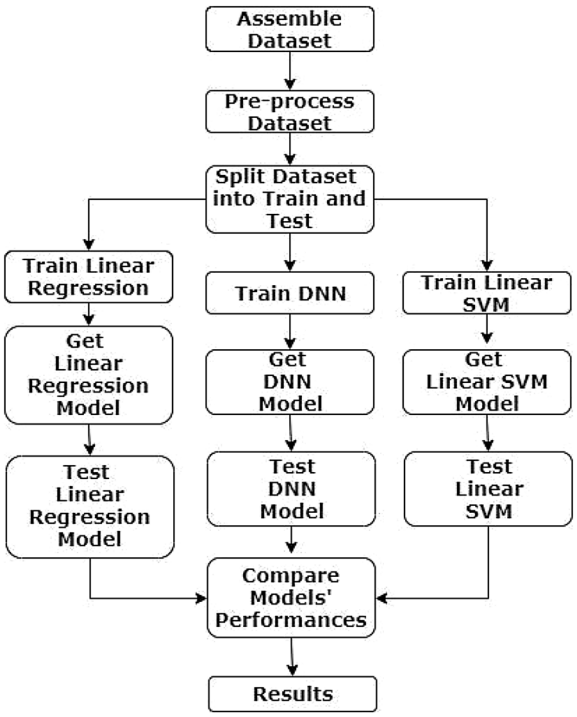

Figure 5. Workflow diagram of the study.

output layers. A DNN obtains the correct numerical manipulation to convert the input into the output.

The workflow diagram of the study is shown in Figure 5. Two traditional regression approaches, namely linear regression and linear support vector machine (SVM), were also performed for comparison with the prediction performance of our proposed DNN. Linear regression is a linear approach that explains the link between a dependent variable and one or more independent variables (Freedman 2009). Reservoir temperature is considered to be the dependent in this study. SVM is a popular regression ML tool developed by Vapnik (1995). It was originally developed as a binary classifier and was later extended to solve regression problems, and it has lately gained much attention as a promising ML with robust mathematical model (Vapnik 1998; Ghaibeh et al. 2006). SVM regression is considered a non-parametric technique because it relies on kernel functions. The main advantage of linear SVM regression over other ML algorithms is that it has good generalization ability.

Overview of Methodology and Dataset

In this study, 83 thermal springs and geothermal wells at different temperatures were selected for the creation of a dataset in Western Anatolia. These springs and geothermal wells are generally located in the Aegean Extension Zone, a tectonic zone in Turkey with large graben systems that include high-, medium- and low-temperature geothermal fields.

After the selection of thermal springs, detailed physical and chemical analyses were conducted based on various references. Some critical parameters were selected for this study that may indicate water–rock interaction and deep recharge for the selected thermal springs. These parameters are temperature of springs, Ph, electrical conductivity (EC), and Na^+, K^+, B_{total}, Cl^- ions and SiO_2 concentrations.

The concentrations of these ions are largely controlled by their supply to the fluid. It is not surprising to have high concentrations of these ions in geothermal fluids, which may extract the constituents from either the enclosing rock or a degassing magma heat source (Nicholson 1993). Na^+ and K^+ ion concentrations are important for understanding water–rock interaction at high temperatures. High B concentration generally points to deep feeding and a high-temperature reservoir at depth (Nicholson 1993). For example, B concentrations of geothermal waters in Kızıldere (Denizli) and Germencik (Aydın) range from 30 to 50 ppm, which reflect a high-temperature geothermal system with 230–245 °C reservoir temperature, while B concentrations of 1–2 ppm were measured at low-temperature natural springs in Turkey (Karakus and Şimsek 2013). Chloride (Cl^-) is one of the representative major anions, and it increases the salinity in geothermal waters. Silica concentration is the principal mineral usually involved in temperature, and

Table 1. Training dataset of the study

Sample label	Sample name	Location	Source type	Reservoir temperature (°C)	pH	EC (microS/cm)	K (mg/l)	Na (mg/l)	Boron (mg/l)	SiO_2 (mg/l)	Cl (mg/l)
1	Derman	Balıkesir	Thermal spring	103[a]	8.8	1160	4	227	1.4	50	62
2	Gönen	Balıkesir	Thermal spring	146[a]	8.5	2000	21	430	7.1	132	265
3	Şamlı	Balıkesir	Thermal spring	107[a]	9.0	1440	4	230	2.0	56	845
4	Bozören	Balıkesir	Thermal spring	67[a]	7.2	960	4	40	0.15	19	33
5	Gümeli	Balıkesir	Thermal spring	88[a]	7.5	580	5	23	0.2	34	13
6	Kaynarca	Bursa	Thermal spring	91[a]	6.9	1349	18	198	1.8	38	8
7	Zeynine	Bursa	Thermal spring	87[a]	7.1	558	5	36	0.0	33	7
8	Dümbüldek	Bursa	Thermal spring	131[a]	6.8	1900	72	440	1.7	96	62
9	Esref Efendi	Bursa	Thermal spring	126[a]	7.0	1215	15	168	1.9	87	9
10	Küplüce	Bursa	Thermal spring	87[a]	7.1	582	4	25	0.2	34	3
11	Zeynine2	Bursa	Thermal spring	90[a]	7.0	557	4	23	0.3	36	3
12	Horhor	Bursa	Thermal spring	88[a]	7.1	568	4	24	0.2	34	3
13	Karacakaya	Bursa	Thermal spring	50[a]	6.9	400	2	20	0.0	11	5
14	Ilıcaksu	Bursa	Thermal spring	91[a]	7.4	490	3	24	0.0	37	9
15	Sadağ	Bursa	Thermal spring	118[a]	7.1	1500	7	220	0.0	72	29
16	Ağaçhisar	Bursa	Thermal spring	85[a]	6.7	1250	3	15	0.0	32	10
17	Küçütçetmi	Çanakkale	Thermal spring	102[a]	7.2	800	2	134	0.2	49	27
18	Topraklar	Çanakkale	Thermal spring	91[a]	8.3	1700	5	320	1.3	38	81
19	Çan	Çanakkale	Thermal spring	73[a]	8.1	3300	24	550	5.0	23	234
20	Etili	Çanakkale	Thermal spring	57[a]	7.4	1900	15	590	0.0	14	93
21	Tekkehamam	Denizli	Thermal spring	171[a]	7.9	3700	64	530	0.0	210	90
22	SP1	Denizli	Thermal spring	185[a]	6.9	4870	94	865	17	270	95
23	SP2	Denizli	Thermal spring	154[a]	7.9	3680	114	870	11	155	85
24	SP3	Denizli	Thermal spring	183[a]	6.9	3000	86	686	16	259	78
25	SP4	Denizli	Thermal spring	154[a]	6.5	3980	75	586	10	154	73
26	SP6	Denizli	Thermal spring	159[a]	6.4	4730	50	535	9	170	134
27	SP8	Denizli	Thermal spring	146[a]	6.2	3850	65	583	8.6	132	145
28	İn mağarası	Denizli	Thermal spring	206[a]	6.5	4401	73	564	13.0	375	87
29	Yenicehamamı	Denizli	Thermal spring	133[a]	5.8	1950	42	260	3.2	100	34
30	Gölemezli	Denizli	Thermal spring	156[a]	6.3	2700	56	540	7.5	160	90
31	Karahayıt	Denizli	Thermal spring	106[a]	6.3	2880	21	120	2.2	55	29
32	Pamukkale Mis	Denizli	Thermal spring	97[a]	7.7	2500	22	130	2.7	43	34
33	Pamukkale Kayna	Denizli	Thermal spring	106[a]	6.2	2340	48	38	0.9	55	15
34	Babacık	Denizli	Thermal spring	148[a]	6.2	3120	113	860	9.2	136	93
35	Balçova	İzmir	Thermal spring	133[a]	8.1	1388	41	239	8.5	100	142
35	Doğanbey	İzmir	Thermal spring	102[a]	7.6	10,330	155	1810	9.4	49	3150
36	Dikili Çoban	İzmir	Thermal spring	125[a]	9.1	2590	33	575	9.0	85	98
37	Dikili Kocaoba	İzmir	Thermal spring	122[a]	8.7	2360	11	310	0.4	80	43
38	Dikili Güzellik	İzmir	Thermal spring	103[a]	8.9	3600	5	375	1.0	51	37
39	Bayındır	İzmir	Thermal spring	109[a]	6.7	970	9	240	0.7	58	18
40	Urganlı	Manisa	Thermal spring	111[a]	8.4	1650	46	520	8.9	62	71
41	Urganlı Uyuz	Manisa	Thermal spring	113[a]	8.0	1755	48	560	7.4	64	71
42	Urganlı Kuru	Manisa	Thermal spring	94[a]	8.4	1770	48	540	8.7	40	76
43	Urganlı Garkın	Manisa	Thermal spring	105[a]	7.0	2260	65	503	13.6	53	62
44	Sart	Manisa	Thermal spring	118[a]	7.6	907	24	198	16.0	72	37
45	Sarıkız	Manisa	Thermal spring	79[a]	8.0	1558	13	240	17.4	27	58
46	Saraycık	Manisa	Thermal spring	153[a]	7.2	3800	106	1020	11.0	150	127
47	Bozöyük	Muğla	Thermal spring	115[a]	7.9	1400	19	148	0.7	68	38
48	KD42	Denizli	Well	244[b]	8.5	5480	191	1464	30	460	144
49	KD46	Denizli	Well	181[b]	8.2	5090	99	1332	19	261	212
50	KD45	Denizli	Well	232[b]	7.9	5770	140	1513	33	492	212
51	KD50	Denizli	Well	218[b]	7.3	5370	140	1389	29	444	248
52	KD55	Denizli	Well	236[b]	7.5	5890	140	1508	31	503	326
53	KD15	Denizli	Well	206[b]	8.7	4790	118	1225	19	257	99
54	KD16	Denizli	Well	209[b]	8.6	4840	125	1240	19	258	99
55	KD20	Denizli	Well	204[b]	8.8	4950	128	1273	20	310	101

Table 1. continued

Sample label	Sample name	Location	Source type	Reservoir temperature (°C)	pH	EC (microS/cm)	K (mg/l)	Na (mg/l)	Boron (mg/l)	SiO_2 (mg/l)	Cl (mg/l)
56	KD21	Denizli	Well	205[b]	8.1	4490	108	1149	14	263	85
57	R3	Denizli	Well	190[b]	8.1	4640	78	1229	15	219	121
58	KD23B	Denizli	Well	245[b]	7.2	5440	179	1415	25	434	118
59	KD23D	Denizli	Well	238[b]	7.1	5250	175	1341	25	431	109
60	KD18A	Denizli	Well	215[b]	7.0	4920	154	1254	24	351	101
61	KD2A	Denizli	Well	237[b]	7.4	4990	159	1239	24	450	103
62	KD9A	Denizli	Well	225[b]	7.0	4910	154	1269	26	381	101
64	R1A	Denizli	Well	231[b]	7.6	4360	118	1099	20	290	89
65	R1	Denizli	Well	220[b]	7.6	4990	153	1318	23	405	102
66	R3A	Denizli	Well	243[b]	7.2	5330	182	1417	29	455	113

[a]Reservoir temperature was calculated by Fournier 1977 for thermal springs
[b]Measured reservoir temperatures for wells. Data were taken from Avsar and Altuntas (2017), Haklidir Tut et al. (2015), Haklidir Tut (2007), MTA (2005), Gökgöz (1998)

Table 2. Testing dataset of the study

Sample label	Sample name	Location	Source type	pH	EC (microS/cm)	K (mg/l)	Na (mg/l)	Boron (mg/l)	SiO_2 (mg/l)	Cl (mg/l)
67	İmamköy	Aydın	Thermal spring	7.4	1772	84	51	0.0	43	25
68	Güre	Balıkesir	Thermal spring	9.1	1300	5.5	265	2.7	38	71
69	Ayvalık Ilıca	Balıkesir	Thermal spring	8.7	1000	0.8	2.6	0.5	30	59
70	Sındırgı	Balıkesir	Thermal spring	7.6	350	0.8	10	0.5	12	10
71	Kükürtlü	Bursa	Thermal spring	7.3	816	18	194	1.9	40	8
72	Oylat	Bursa	Thermal spring	7.6	1450	4.3	23.5	0.0	42	14
73	Hıdırlar	Çanakkale	Thermal spring	8.1	700	4.0	110	0.7	51	19
74	SP9	Denizli	Thermal spring	6.6	4120	75	564	10	184	98
75	Tekkehamam2	Denizli	Thermal spring	7.7	3800	99	984	20	160	97
76	Kükürtlü	Manisa	Thermal spring	7.1	1880	8.0	98	7.6	30	31
77	Tekkeköy	Denizli	Thermal spring	7.6	4500	95	995	12	251	90
78	KD54	Denizli	Well	7.2	5090	140	1225	38	426	180
79	KD14	Denizli	Well	8.9	4890	129	1257	20	292	100
80	KD22	Denizli	Well	8.3	4750	126	1225	17	258	92
81	R6	Denizli	Well	8.4	4590	117	1258	21	249	94
82	R5A	Denizli	Well	7.5	4680	131	1232	22	650	95
83	K5	Denizli	Thermal spring	7.5	4500	74	1126	12	191	90

the solubility of SiO_2 decreases with a decrease in temperature in a geothermal system. Silica in thermal water tends to precipitate when temperature decreases, which directly affects the quality of sampling and ability to analyze real silica concentration in thermal water. Silica is an important mineral for

Table 3. Ground-truth data

Sample label	Sample name	Source type	Reservoir temperature (°C)
67	İmamköy	Thermal spring	97
68	Güre	Thermal spring	92
69	Ayvalık Ilıca	Thermal spring	83
70	Sındırgı	Thermal spring	53
71	Kükürtlü	Thermal spring	94
72	Oylat	Thermal spring	96
73	Hıdırlar	Thermal spring	103
74	SP9	Thermal spring	164
75	Tekkehamam2	Thermal spring	156
76	Kükürtlü	Thermal spring	83
77	Tekkeköy	Thermal spring	183
78	KD54	Well	225
79	KD14	Well	208
80	KD22	Well	201
81	R6	Well	207
82	R5A	Well	230
83	K5	Thermal spring	190

calculation of reservoir temperatures in thermal springs, and the precipitation of silica can affect the calculation. The amount of dissolved ions in geothermal fluids is the result of temperature and reservoir geology in a region. Low-temperature fluids contain smaller amounts of dissolved solids compared to higher-temperature geothermal fluids, and EC is quite an important parameter for detecting dissolved solids in geothermal fluids (Nicholson 1993).

Three datasets were compiled in this study: one for training, one for testing and one set of ground truth data. Of 83 thermal springs and geothermal wells, 66 were selected for the training set (Table 1) and 17 for the testing set (Table 2). The ground truth data contain reservoir temperatures calculated by geothermometers for thermal springs and measured reservoir temperatures for geothermal wells in the testing dataset (Table 3). Different silica geothermometers were applied to thermal springs; however, the quartz adiabatic geothermometer (Fournier 1977) is the most suitable, and so it was used for the calculation of reservoir temperatures of thermal springs.

RESULTS AND DISCUSSION

Geothermal Reservoir Temperature Prediction by Using Regression

ML models were trained and evaluated using the regression approach based on the training dataset (Table 1). The results show the relationship between the actual geothermal reservoir temperatures and the predicted geothermal reservoir temperatures for the training model. Figure 6 includes the location numbers against geothermal reservoir temperature plots for the three regression algorithms under consideration, covering both actual and predicted reservoir temperatures. The variations between actual and predicted reservoir temperatures are depicted in the graphics in Figure 6. If actual and predicted points coincide, the maximum accuracy is indicated. The root-mean-square error (RMSE) and mean absolute error (MAE) for the training data using linear regression, linear SVM and DNN models are given in Table 4.

In Figure 7, reservoir temperatures predicted using the training dataset (Table 1) are plotted against the actual reservoir temperatures, true response, in the form of a regression line. The performance plots of the three algorithms are presented. The vertical distance from the regression line to any point is the error of the prediction. Maximum points on the regression line indicate the most accurate algorithm.

Linear regression, linear SVM and DNN models were tested using the testing dataset (Table 2). The results given in Table 5 and included in the graphs show the relationship between actual geothermal reservoir temperatures and predicted geothermal reservoir temperatures for the testing dataset. RMSE and MAE values for the testing dataset using linear regression, linear SVM and DNN models appear in Table 6 and Figure 8.

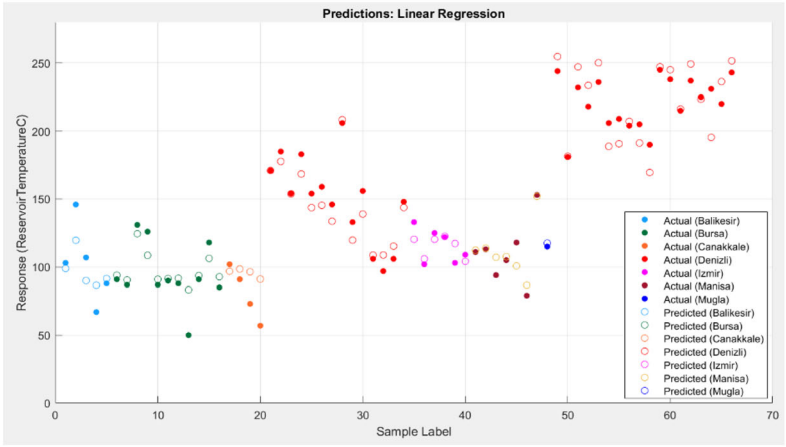

(a) Linear Regression

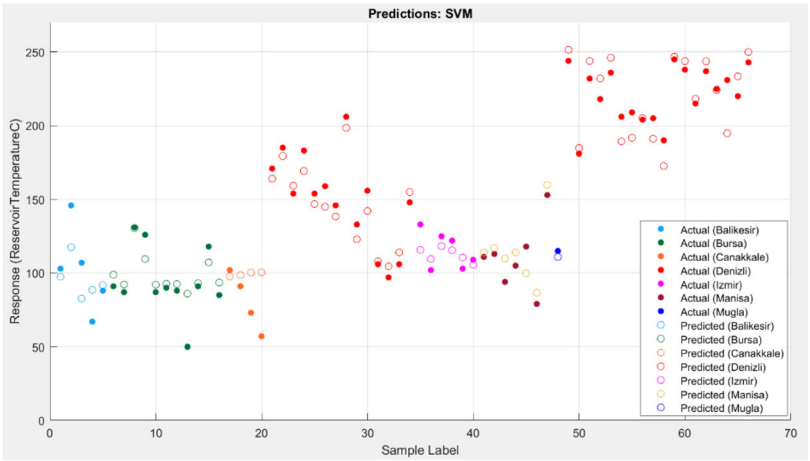

(b) Linear SVM

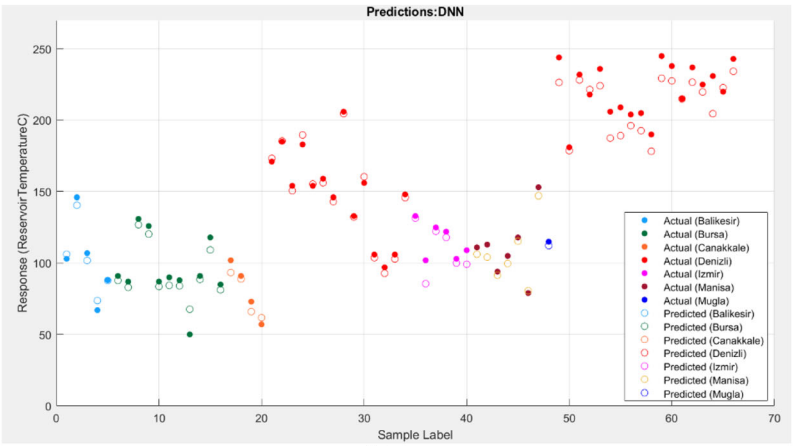

(c) DNN

Figure 6. Response plots. Visualizations of location vs. reservoir temperatures covering both the actual and predicted values by (a) linear regression, (b) linear SVM and (c) DNN.

Table 4. RMSE and MAE for linear regression, linear SVM and DNN models using the training dataset

	Linear regression	Linear SVM	DNN
Root-mean-square error (RMSE)	16.05	17.58	10.24
Mean absolute error (MAE)	10.68	12.40	7.96

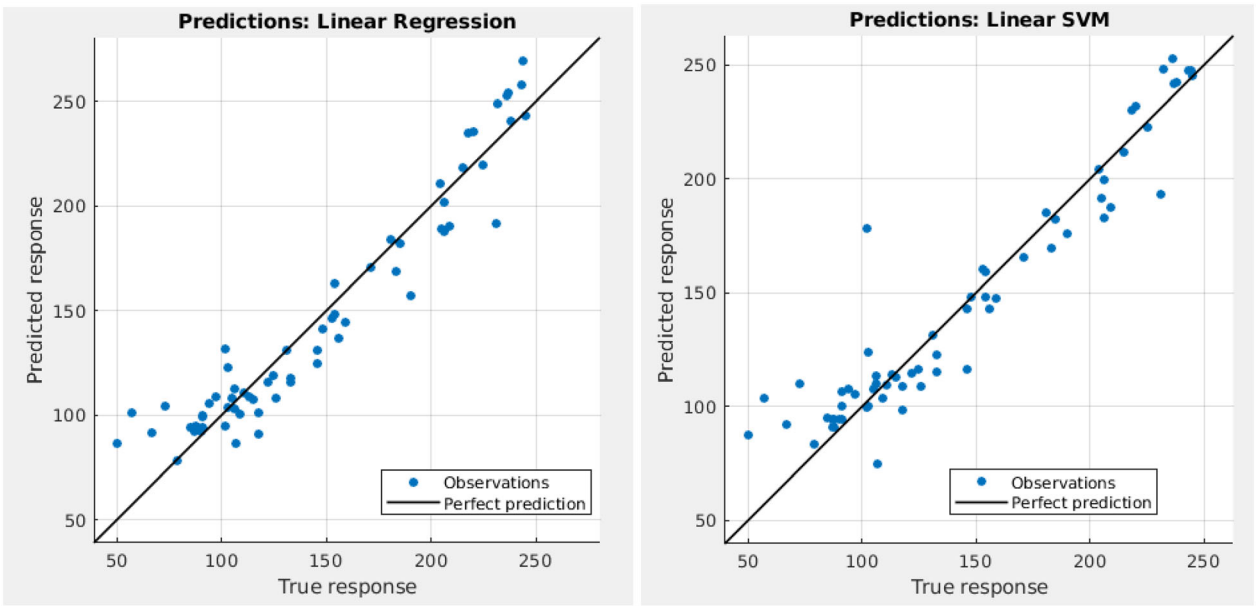

(a) Linear Regression **(b)** Linear SVM

(c) DNN

Figure 7. Visualization of actual reservoir temperatures vs. predicted temperatures by (a) linear regression modeling, (b) linear SVM modeling and (c) DNN modeling.

Table 5. Measured (actual) and predicted reservoir temperatures

Sample label	Location	Type	Reservoir temperature (°C)	Prediction (linear regression)	Prediction (linear SVM)	Prediction (DNN)
İmamköy	Aydın	Thermal spring	97	121.90	119.98	100.44
Güre	Balıkesir	Thermal spring	92	100.31	98.66	92.39
Ayvalık Ilıca	Balıkesir	Thermal spring	83	97.19	93.47	87.60
Sındırgı	Balıkesir	Thermal spring	53	85.63	87.48	73.59
Kükürtlü	Bursa	Thermal spring	94	97.10	100.67	86.29
Oylat	Bursa	Thermal spring	96	100.36	99.06	84.86
Hıdırlar	Çanakkale	Thermal spring	103	100.31	100.07	91.29
SP9	Denizli	Thermal spring	164	155.52	154.59	158.59
Tekkehamam2	Denizli	Thermal spring	156	148.69	151.94	167.84
Kükürtlü	Manisa	Thermal spring	83	91.43	92.33	84.52
Tekkeköy	Denizli	Thermal spring	183	182.13	181.50	190.83
KD54	Denizli	Well	225	222.70	218.79	224.45
KD14	Denizli	Well	208	202.45	199.06	200.29
KD22	Denizli	Well	201	191.45	191.01	200.87
R6	Denizli	Well	207	183.06	183.52	199.01
R5A	Denizli	Well	230	296.78	285.42	231.38
K5	Denizli	Thermal spring	174	158.50	162.59	168.28

Table 6. RMSE and MAE for linear regression, linear SVM and DNN models using the testing dataset

	Linear regression	Linear SVM	DNN
Root-mean-square error (RMSE)	21.13	18.94	8.29
Mean absolute error (MAE)	14.05	13.35	6.45

The objective of the study was to determine the algorithm that would give the lowest RMSE. Based on the results, the DNN algorithm generates the least error (Tables 4 and 6). In this study, the DNN model provides results that are more satisfactory compared to the traditional ML techniques, namely linear regression and linear SVM, for the geothermal reservoir temperature prediction. The DNN model provides more accurate values and gives values closer to geothermometer calculations for reservoir temperature overall. It provides especially good results for sample IDs 1, 2, 11, 36, 54, 64, 71 and 82. Although the DNN model's accuracy directly depends on the quality of the hydrogeochemical data, it provides coherent results for medium–high-temperature geothermal reservoirs. In this study, the reservoir temperatures of geothermal wells predicted by using DNN based on a few hydrochemical data points look impressive in that there is only 1 °C difference between the predicted and measured reservoir temperatures for the KD22, KD54 and R5A wells. Another interesting finding is about the K5 thermal spring. This spring's measured temperature was around 72.5 °C (MTA 2005), and the silica geothermometer calculation gives 174 °C for the reservoir. The DNN model predicted the reservoir temperature as 168 °C and showed similar hydrogeochemical characterization to the KD13

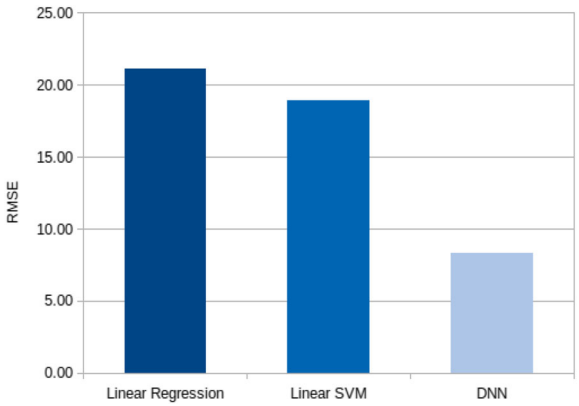

Figure 8. Visualization of RMSE for linear regression, linear SVM and DNN models using the testing dataset.

well, which uses the same reservoir in Sarayköy, Denizli (Zorlu 2009).

CONCLUSION

In this study, natural thermal springs and geothermal wells were selected as a dataset from different geothermal systems in Western Anatolia. Of the total 83 thermal springs, 66 were selected for training dataset analysis and 17 for the testing dataset. The different ML algorithms were evaluated using the same dataset for consistent comparison of results for each algorithm. Neither the linear regression nor the linear SVM algorithms provide satisfactory results for all water samples. In the overall evaluation of the testing results, the DNN algorithm gave the most accurate values. The results show that DNN is capable of predicting reservoir temperatures accurately based on typical hydrogeochemical parameters, namely EC, Na+, K+, boron, Cl− and silica (or without silica) for most geothermal springs. This can be especially important for medium-temperature geothermal springs owing to silica precipitation during the sampling period. For this reason, the DNN model is a new option for predicting reservoir temperatures for such springs. In addition, this approach can be used as an alternative to the pressure temperature spinner (PTS) tool for high-temperature geothermal wells for long-term monitoring of reservoir temperature in geothermal fields. However, because only a limited hydrogeochemical dataset was used for reservoir temperature prediction in this study, it is assumed that more reliable results could be obtained with more data. Using this new approach may provide important information before taking a decision to undertake a new drilling operation in a geothermal field.

REFERENCES

Arnorsson, S. (Ed.). (2000). *Isotopic and chemical techniques in geothermal exploration, development and use* (p. 351). Vienna: International Atomic Energy Agency.

Avsar, Ö., & Altuntas, G. (2017). Hydrogeochemical evaluation of Umut geothermal field (SW Turkey). *Environmental Earth Science, 76,* 582.

Baba, A., Demir, M. M., Koç, G., & Tuğcu, C. (2015). Hydrogeological properties of hyper-saline geothermal brine and application of inhibiting siliceous scale via pH modification. *Geothermics, 53,* 406–412.

Bozkurt, E. (2001). Neotectonics of Turkey—A synthesis. *Geodinamica Acta, 14*(1–3), 3–30.

Bundschuh, J., Maity, J. P., Nath, B., Baba, A., Gündüz, O., Kulp, T. R., et al. (2013). Naturally occurring arsenic in terrestrial geothermal systems of western Anatolia, Turkey: Potential role in contamination of freshwater resources. *Journal of Hazardous Materials, 262,* 951–959.

Fournier, R. O. (1977). Chemical geothermometers and mixing models for geothermal systems. *Geothermics, 5,* 41–50.

Freedman, D. A. (2009). *Statistical models: Theory and practice* (2nd ed.). Cambridge: Cambridge University Press.

Ghaibeh, A. A., Sasaki, M., & Chuman, H. (2006). Using Voronoi grid and SVM linear regression in drug discovery. *2006 IEEE Symposium on Computational Intelligence and Bioinformatics and Computational Biology*, Toronto, Canada.

Gökgöz, A. (1998). Geochemistry of the Kızıldere–Tekkehamam–Buldan–Pamukkale Geothermal Fields, Turkey. Report No. 5: The United Nations University Geothermal Training Programme Orkustofnun, Grensasvegur 9, 18 108 Reykjavik, Iceland (pp. 115–156).

Haklidir Tut, F. S. (2007). Geochemical study of thermal, mineral and groundwater in Bursa city and surroundings. *Ph.D. thesis*, Dokuz Eylul University, Izmir, pp. 328 (in Turkish).

Haklidir Tut, F. S. (2013). Hydrogeochemical Evaluation of thermal, mineral and cold waters between Bursa City and Mount Uludağ in the South Marmara Region of Turkey. *Geothermics, 48,* 132–145.

Haklidir Tut, F. S. (2015). Geothermal energy sources and geothermal power plant technologies. *Energy Systems and Management, Springer Energy Proceedings, 11,* 115–124.

Haklidir Tut, F. S. (2017). Scaling types and systems used to provide controlling of scale occurrence in high temperature geothermal systems in Western Anatolia. *Geological Bulletin of Turkey, 60,* 363–382. **Turkish**.

Haklidir Tut, F. S., & Haklidir, M. (2017). Fuzzy control of calcium carbonate and silica scales in geothermal systems. *Geothermics, 70,* 230–238.

Haklidir Tut, F. S., & Haklidir, M. (2019). The fluid temperature prediction with hydro-geochemical indicators using a deep learning model: A case study Western Anatolia (Turkey). *43rd Workshop on Geothermal Reservoir Engineering Stanford University, CA*, February 11–13.

Haklidir Tut, F. S., & Şengün, R., (2020). Hydrochemical similarities and differences between high temperature geother-

mal systems with similar geologic settings in the Büyük Menderes and Gediz Grabens of Turkey. *Geothermics*, 83 (in press).

Haklidir Tut, F.S., Şengün, R., & Haizlip Robinson, J. (2015). The geochemistry of deep reservoir wells in Kızıldere Geothermal Field (Turkey). *Proceedings of 2015 World Geothermal Congress, Melbourne-Australia*, 19–24 April.

Holtzman, B. K., Pate, A., Paisley, J., Waldhauser, F., & Repetto, D. (2018). Machine learning reveals cyclic changes in seismic source spectra in geysers geothermal field. *Science Advances, 4*(5), 2929.

Karadas, M., & Akkurt, G. G. (2014). Rapid development of geothermal power generation in Turkey. In A. Baba, J. Bundschuh, & D. Chandrasekharam (Eds.), *Geothermal Systems and Energy Sources: Turkey and Greece* (pp. 197–224). Boca Raton: CRC Press.

Karakus, H., & Şimsek, Ş. (2013). Tracing deep thermal water circulation systems in the E-W trending Büyük Menderes Graben, Western Turkey. *Journal of Volcanology and Geothermal Research, 252*(2013), 38–52.

Karingithi, C. W. (2009). Chemical geothermometers for geothermal exploration. Short Course IV on Exploration for Geothermal Resources, organized by UNU-GTP, KenGen and GDC, at Lake Naivasha, Kenya, November 1–22, 2009.

Lindal, B. (1973). Industrial and other application of geothermal energy. In H. Armstead (Ed.), *Geothermal energy* (pp. 135–148). Paris: UNESCO.

MTA. (2005). *Türkiye Jeotermal Kaynaklar Envanteri, prepared by the General Directorate of Mineral Research and Exploration*, Ankara, Turkey, 849 p.

Mutlu, H., & Güleç, N. (1998). Hydrogeochemical outline of thermal waters and geothermometry applications in Anatolia (Turkey). *Journal of Volcanology and Geothermal Research, 85*(1–4), 495–515.

Nicholson, K. (1993). *Geothermal fluids. Chemistry and Exploration Techniques*. xv + 263 pp. Berlin, Heidelberg, New York, London, Paris, Tokyo, Hong Kong: Springer-Verlag. Price DM 138.00, Ös 1076.40, SFr 138.00 (hard covers). ISBN 3 540 56017 3.

Ochieng, L. (2013). Overview of geothermal surface exploration methods. Short Course VIII on Exploration for Geothermal Resources, organized by UNU-GTP, GDC and KenGen, at Lake Bogoria and Lake Naivasha, Kenya, Oct. 31–Nov. 22, 2013.

Parlaktuna, M., Mertoğlu, O., Şimsek, Ş., Paksoy, H., & Basarır, N. (2013). Geothermal country update report of Turkey (2010–2013). European Geothermal Congress 2013 Pisa, Italy, 3–7 June 2013.

Rezvanbehbahani, S., Stearns, A. L., Kadivar, A., Walker, D. J., & Van der Veen, C. J. (2017). Predicting the geothermal heat flux in Greenland: A machine learning approach. *Geophysical Research Letters, 44,* 12271–12279.

Russell, S.J., & Norvig, P., (2010). *Artificial intelligence: A modern approach*, Third Edition, Prentice Hall ISBN 9780136042594.

Şalk, M., Pamukçu, O., & Kaftan, İ. (2005). Determination of the Curie point depth and heat flow from Magsat Data of Western Anatolia. *Journal of Balkan Geophysical Society, 8*(4), 149–160.

Samuel, A. (1959). Some studies in machine learning using the game of checkers. *IBM Journal of Research and Development, 3*(3), 210–229. https://doi.org/10.1147/rd.33.0210.

TJD. (2018). Turkish Geothermal Energy Association website; http://www.jeotermaldernegi.org.tr/.

Topçu, G., Koç, G. A., Baba, A., & Demir, M. M. (2019). The injection of CO_2 to hypersaline geothermal brine: A case study for Tuzla region. *Geothermics, 80,* 86–91.

Vapnik, V. (1995). *The nature of statistical learning theory*. New York: Springer.

Vapnik, V. (1998). *Statistical learning theory*. New York: Wiley.

Zorlu. (2009). *Hydrochemical evaluation of Kızıldere geothermal field and surroundings, report*. İstanbul: Zorlu Energy Company.